Theoretical analysis and experiment of seed-picking mechanism of belt high-speed seed-guiding device for corn

Chengcheng Ma,[1] Shujuan Yi,[1] Guixiang Tao,[1] Yifei Li,[1] Hanwu Liu[2]

[1]College of Engineering, Heilongjiang Bayi Agricultural University, Daqing, Heilongjiang Province;
[2]Debon (Jiamusi) Agricultural Machinery Co., Ltd. Jiamusi, Heilongjiang Province, China

Abstract

Under the condition of high-speed sowing (12-16 km/h) due to the high rotational speeds of the seed disk, the seeds leave the disk at an excessively high speed, which challenges the seed-picking capacity of the belt-type high-speed seed guide device. In this paper, the theory of the seed-picking mechanism is analyzed, and performance optimization tests are completed to further improve the operation effect of the seeder. The mechanical model of seed picking was established through the force analysis of seeds. The influence of vacuum degree, feeder wheel rotation speed, and seed-picking angle on seed-picking quality and the parameter range of each factor were obtained by single factor test. A three-factor five-level quadratic orthogonal rotation combination test was performed, and the test results were refined and evaluated. The test factors used were vacuum degree, feeder wheel rotation speed, and seed-picking angle. The test indexes used were the seed-picking rate, re-picking rate, and miss-picking rate. According to the results, the seed-picking rate was 99.89%, the re-picking rate was 0, and the miss-picking rate was 0.11% when the vacuum degree was 6.89KPa, the feeder wheel rotation speed was 568.95rpm, and the seed-picking angle was 7.6°.

Correspondence: Shujuan Yi, College of Engineering, Heilongjiang Bayi Agricultural University, Daqing, Heilongjiang Province, China.
E-mail: yishujuan_2005@126.com

Key words: high-speed sowing of corn; high-speed camera technology; seed-picking mechanism; test.

Acknowledgments: this work was supported by The National Natural Science Foundation of China (Grant No. 52275246) and "100 Million" Major Project of Engineering Science and Technology (Grant No. 2020ZX17B01-3).

Contributions: the authors contributed equally.

Conflict of interest: the authors declare no potential conflict of interest.

Funding: none.

Received: 3 November 2022.
Accepted: 4 March 2023.

Journal of Agricultural Engineering 2023; LV:1543
doi:10.4081/jae.2023.1543

Introduction

Because of its powerful capacity to control seeds, the belt corn seed guide device is frequently utilized for high-speed corn sowing (Jinqing *et al.*, 2016). It must pass through the seed-picking mechanism on its way from the seed disk to the seed guide belt, and the quality of seed picking directly affects the quality of the succeeding seed guide (Kocher *et al.*, 2011; Liu *et al.*, 2019). Therefore, this paper studies the seed-picking mechanism of the belt-type corn high-speed seed-guiding device and optimizes its performance in order to further improve the operating effect of corn seeders in high-speed sowing.

There are three primary types of corn seed-picking mechanisms, according to some studies (Badua *et al.*, 2021; Qi *et al.*, 2018). The first type is the spoon-type seed-picking mechanism used in corn hole seeders (Xu *et al.*, 2020; Xiong *et al.*, 2021; Wang *et al.*, 2021). A spoon-type seed-picking mechanism was created by using the seed spoon as its primary working component (Hanna *et al.*, 2010) With a duckbill hole seeder, it is simple to use and have stable performance. However, the structural characteristics of the seed spoon have a significant impact on the seed picked, and the hole seeder is unable to operate under high-speed sowing (Li *et al.*, 2020). In order to achieve precision seeding of different diameter seeds without changing the roller, Kaixing, *et al*. (2020) developed a variable-size pneumatic cylinder precision seed-picking mechanism. However, this device was only suitable for low-speed seeding. The second type is the seed-picking device carried by the seed disk in the seeding apparatus, which is divided into spring finger clamping and magnetic finger clamping (Patel *et al.*, 2019). By using a spring finger clamp device, Jin-Wu *et al*. investigated the movement law of corn seeds and improved the finger clamp's structural design (Jinwu *et al.*, 2017). To increase the stability of seed metering performance, Liu *et al.* (2021) created a magnetic pickup finger seed metering device that uses magnetic force to open and close the pickup finger. The fast-sowing speed, however, easily results in the unstable clamping of corn seeds, which can't meet the requirements of high-speed sowing. The third type is the seed-picking mechanism used in the air-suction seeding apparatus. The brush seed guide belt created by the John Deere Company is an example. As soon as the corn seeds are released from the air-suction seeding device, they immediately

stick to the brush belt, allowing the brush belt to pick them up and transport them downward. However, under continuous high-speed operation, the brush belt is vulnerable to wear (Garner *et al.*, 2010; 2016). The feeder wheel is used as the seed-picking component in a speed tube created by Precision Planting Company, but the feeder wheel's structure is intricate and the theory of seed-picking is not perfect (Sauder *et al.*, 2002). Given the above problems, according to the agronomic requirements of corn sowing, this paper: i) establishes the mechanical model of seed picking with the feeder wheels through the dynamic analysis of seeds, and the parameters influencing the effect of seed picking were discovered; ii) records the seed movement trajectories in various movement states at a speed of 12-16 km/h by using high-speed camera technology, and the seed trajectory change rules were also obtained; iii) gets the best parameter combination for the seed-picking mechanism by the orthogonal rotation combination test.

Materials and Methods

Structure characteristics of the seed-picking mechanism

The device's overall structure is primarily made up of a seed conveying belt, feeder wheels, seed throwing plate, pre-tightening spring, seed cleaning claw, driving pulley, driven pulley, motor, seed protection cover, gear box, and seed conveying belt shell, as shown in Figure 1. The device's working process is broken down into three stages: seed picking, seed transporting, and seed throwing. The primary feeder wheel, auxiliary feeder wheel, seed cleaning claw, gear shafts, gear box, front shell, and rear cover shell are the main components of the seed-picking mechanism of the belt high-speed seed-guiding device which is depicted in Figure 2. The primary feeder wheel and the auxiliary feeder wheel have a radius ratio of 1.7:1 and are made of rubber material. The inclined arc structure fingers are evenly distributed around the feeder wheel, with 15 fingers on the auxiliary feeder wheel and 17 fingers on the primary feeder wheel.

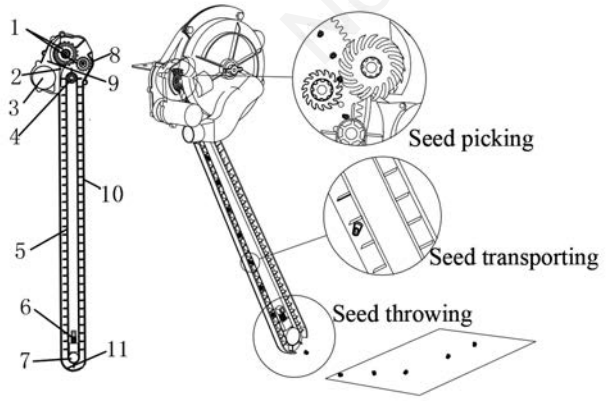

Figure 1. Assembly structure of air-suction seeding apparatus and belt-type corn high-speed seed guiding device. 1) Feeder wheels; 2) seed cleaning claw; 3) motor; 4) driving pulley; 5) seed conveying belt; 6) pre-tightening spring; 7) driven pulley; 8) gear box; 9) seed protection cover; 10) seed conveying belt shell; 11) seed throwing plate.

Principle of operation

The seed-picking mechanism is installed at the side of the seed disk, and the feeder wheels pick down the corn seeds before the seeds are separated from the seed disk. After that, they are transferred and released into the bottom seed guiding belt. Clamping corn seeds (I), transporting corn seeds (II), and releasing corn seeds (III) are the three distinct working phases that make up the seed-picking process, as shown in Figure 3. The motor drives the gear, which forces the primary and auxiliary feeder wheels to rotate in opposite directions when picking seeds. The rotating speed ratio of the primary and auxiliary feeder wheels is 1.79. When the corn seeds carried by the seed disk move to the seed-picking port, the primary and auxiliary feeder wheels pick the corn seeds by rotating and clamping. The rotational clamping of the feeder wheels causes the clamped seeds to migrate downward. The seeds are then released by the feeder wheels into the bottom seed guide belt's seed cavity. By employing this seed-picking technique, the corn seeds can be released from the seeding apparatus and allowed to fall onto the seed guide belt without suffering any damage, guaranteeing the stability of the seed flow even at high speeds.

Mechanical analysis and parameter determination

The corn seeds go through two stages: the first is when they come into touch with the feeder wheels, and the second is when the feeder wheels clamp and move the corn seeds.

Instantaneous force analysis of contact between seeds and feeder wheels

Only the corn seeds' gravity G, the supporting forces F_{N1} and F_{N2} of the feeder wheels on the corn seeds, and the elastic force F_t of the feeder wheels on the corn seeds are acting on the corn seeds when they come into contact with the feeder wheels. The coordinate system is established by taking the center point of the corn seed circle as the coordinate origin, as shown in Figure 4. Figure 5 displays the stress diagram of corn seeds in this state.

Assuming that the elasticity of the primary feeder wheel and the auxiliary feeder wheel to the corn seeds is the same, the stress equation for corn seeds is shown in Eq. (1).

$$\begin{cases} (F_{N1}+F_t)\sin\theta_1+(F_{N2}+F_t)\sin\theta_2=G \\ (F_{N1}+F_t)\cos\theta_1=(F_{N1}+F_t)\cos\theta_2 \\ F_t=k\cdot\Delta x \end{cases} \quad (1)$$

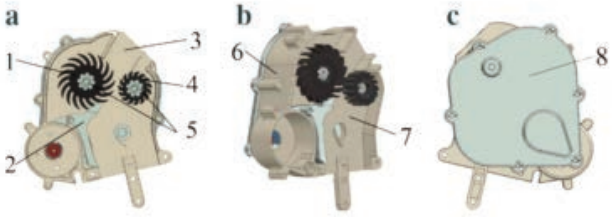

Figure 2. Structure characteristics of the seed-picking mechanism. **a**) Front view; **b**) axonometric view; **c**) back view. 1) Primary feeder wheel; 2) seed cleaning claw; 3) seed-picking entrance; 4) auxiliary feeder wheel; 5) gear shafts; 6) gear box; 7) front shell; 8) rear cover shell.

When the feeder wheels apply a clamping force to corn seeds, the primary and auxiliary feeder wheels immediately produce friction forces on the corn seeds, and the sum of these friction forces is the clamping force of the feeder wheels to the corn seeds, as shown in Eq. (2).

$$\begin{cases} f_1 = \mu \dfrac{G\cos\theta_2 + k^2x^2(\cos\theta_2 - \cos\theta_1)(\sin\theta_2 + \tan\theta_1\cos\theta_2)^2}{k^2 \cdot \Delta x^2(\sin\theta_2 + \tan\theta_1\cos\theta_2)^2\cos\theta_1} \\ f_2 = \mu \dfrac{G}{k^2 \cdot \Delta x^2(\sin\theta_2 + \tan\theta_1\cos\theta_2)^2} \\ F_C = \sqrt{f_1^2 + f_2^2 + 2f_1f_2\cos(\theta_1 + \theta_2)} \end{cases} \quad (2)$$

The feeder wheel's clamping force on seeds has an impact on the effect of picking seeds. Eq. (2) shows that the seed-picking angle, the elastic coefficient of the feeder wheels, and the finger distortion all have an impact on the clamping force. The elastic coefficient and finger distortion can be disregarded, though, because the corn seeds are barely in contact with the feeder wheels and the form variable of a finger is minimal.

Force analysis on the process of moving seeds by feeder wheels

When the seed enters between the two feeder wheels and is transported, the total friction provided by the feeder wheels is clamping force. Currently, the force on the seed is shown in Figure 6. It is affected by the clamping force of the feeder wheel on the seed Fc, the centrifugal force J, the supporting force N of the hole, adsorption force P and the gravity G of the seed itself. To ensure that the seeds are taken down, it is necessary that when the seeds are transported to the center line of the two feeder wheels, the clamping force of the feeder wheel on the seeds is greater than the sum of T (the resultant force of seed gravity G and centrifugal force J) and N' (the supporting force of the hole on the seed along the direction of the parallel seed disk), as shown in Eq. (3).

$$F_c > T + N' \quad (3)$$

The centrifugal force J, a supporting force of the hole on the seed along the direction of the parallel seed disk N', adsorption force P and T (resultant force of seed gravity G and centrifugal force J) are as follows:

$$\begin{cases} T = J \cdot G\sin\tau \\ J = mR\omega^2 \\ N' = N_c \cdot P \\ P = (\pi d^2/4)(P_a - P_0) \end{cases} \quad (4)$$

By substituting formula (4) into formula (3), it can obtain the Eq. (5):

$$F_c > mR\omega^2 \cdot G \cdot \sin\tau + N_c(\pi d^2/4)(P_a - P_0) \quad (5)$$

It can be known from Eq. (5) that when the structure parame-

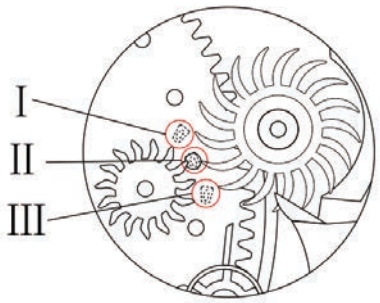

Figure 3. . Schematic diagram of working principle. I) Clamping corn seeds; II) transporting corn seeds; III) releasing corn seeds.

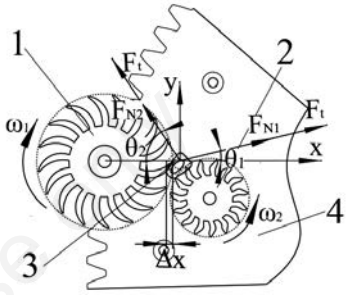

Figure 4. Schematic diagram of seed just touching feeder wheel. 1) Primary feeder wheel; 2) auxiliary feeder wheel; 3) seed; 4) seed disk.

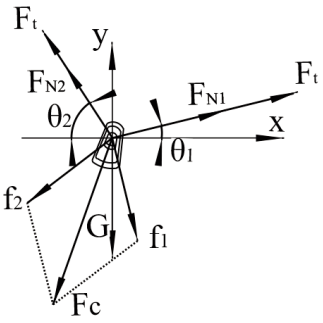

Figure 5. Force at the moment of contact with seed feeder wheel.

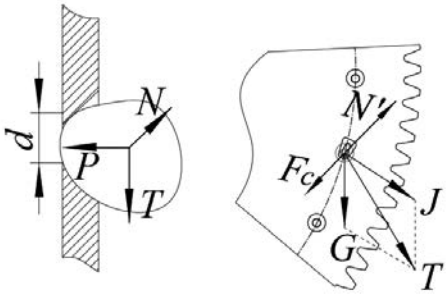

Figure 6. Force during the movement of the seed by the feeder wheels.

ters of the seed apparatus are constant, the clamping force is affected by the feeder wheel rotation speed and the vacuum degree.
To sum up, it can be seen from the established mechanical model (Equations 2 and 5) that the factors affecting the clamping force of the feeder wheel on seeds are the angle of seed taking, the feeder wheel rotation speed and the vacuum degree.

Test conditions and materials

The test device makes use of belt high-speed seed-guiding device and air-suction seeding equipment that Precision Planting developed. Transparent 3D printing technology is used to create the shell, sealed chamber, and seed disk of the seeding apparatus, enabling convenient observation of the seed-picking status of the feeder wheels (Figure 7). Through the pre-tests, the 18-hole seed disk was chosen as the test's seed disk. The detecting tool is a computer-controlled high-speed camera system of a PCO.dimaxCS3 camera. The two major components of the high-speed camera system are a high-speed digital camera for capturing the passage of corn seeds and a computer for data processing and monitoring.
The high-speed digital camera is set to a 500 frame rate, and the time interval between succeeding photos is set to 2 ms in order to produce the graphic resolution of the corn seed movement trajectories suitable for the seed-picking mechanism. Choose pixels with a 1920×1440 pixel image size. Build the test bench as indicated in Figure 8 by positioning the camera at the same horizontal height as the feeder wheel and aiming at the transparent front shell of the seed taking port. The fan's negative pressure is 7 KPa. In the test, the Demeiya No. 1 corn seed variety was chosen. The 1000-grain weight was 299.6g, the form was half horseshoe, the color of the corn seed was yellow, and the moisture content was 12.3%.

Test method

The displacement curve of corn seeds is derived through the post-processing module of the high-speed camera system. Each series of tests was conducted three times, with the rotating speed of the seed disk during shooting being 39, 42, 47, 50, and 53rpm (equivalent to the advancing speed of the seeding operation being 12, 13, 14, 15, and 16km/h, respectively). Figure 9 depicts the process of clamping, transporting, and releasing corn seeds with the feeder wheels while being captured by the high-speed camera. As seen in Figure 10, the high-speed camera system's post-processing module generates the movement trajectories of corn seeds in different motion states. The displacement curves of the seeds in Figure 10a-b are smooth during the time range of 0-1.5 s, which suggests that the seed disk is responsible for the movement of the seeds at this point. The displacement curve of the seeds remained smooth during the 1.5-2.0 s in Figure 10a, showing that the feeder wheels were handling and moving the seeds. The displacement curve of the seeds is wavy in Figure 10b during the 1.5-2.0 s period, indicating that the feeder wheels did not pick the seeds but rather repeatedly collided and bounced with them instead.

Test factors and indexes

The vacuum degree of the seeding apparatus, the feeder wheel rotation speed, and the seed-picking angle are the main factors affecting the seed-picking quality, according to the previous theoretical analysis, pre-test, and actual production experience. To test these three factors, single-factor tests and orthogonal optimization tests will be conducted. The feeder wheel rotation speed and the vacuum degree will be controlled by adjusting the speed control knob of the speed regulator, respectively. The seed-picking angle is controlled by adjusting the relative angle between the primary

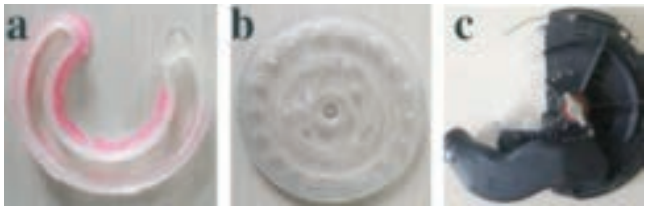

Figure 7. Seeding apparatus parts with transparent treatment. **a**) Sealed chamber; **b**) seed disk; **c**) shell of seeding apparatus.

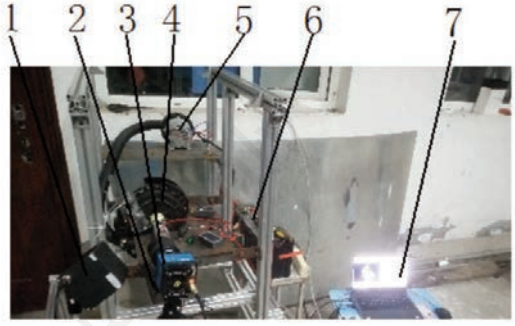

Figure 8. Seed-picking performance test bench under high-speed camera. 1) LED lighting; 2) seed-picking mechanism; 3) high-speed camera; 4) air-suction seeding apparatus; 5) fan; 6) battery; 7) computer.

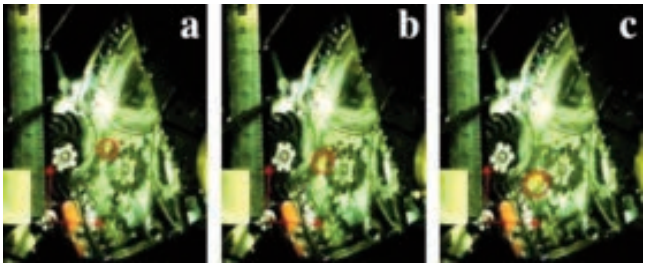

Figure 9. Process of seed-picking under high-speed camera. **a**) Clamping seed; **b**) transporting seed; **c**) releasing seed.

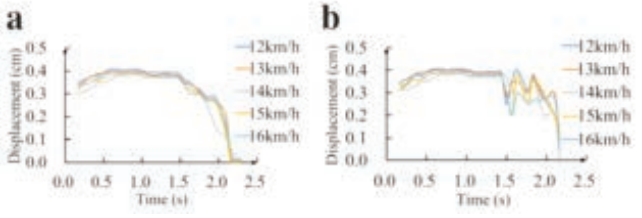

Figure 10. Movement trajectories of seeds in different motion states.

and auxiliary feeder wheels and the axis of the seed metering disc, so as to ensure the operability and accuracy of the test.

Selecting the seed-picking rate, the re-picking rate, and the miss-picking rate as the test indexes, and the computing formulas is shown in Eq. (6).

$$\begin{cases} S = \frac{n_1}{N} \times 100\% \\ M = \frac{n_2}{N} \times 100\% \\ H = \frac{n_3}{N} \times 100\% \end{cases} \quad (6)$$

Determination of parameter range of factors

Single factor tests can be used to determine the effective range of parameters for each factor, and their changing dynamics can be analyzed. Pre-tests from multiple groups, sowing requirements in practice, and the range of variables that can be controlled effectively suggest that the vacuum degree is between 6 KPa and 8 KPa, the feeder wheel rotation speed is between 520 rpm and 660 rpm (The rotation speed of the feeder wheel here refers to the rotation speed of the primary feeder wheel), and the seed taking angle is between 6° and 20°. The seed disk rotated at a speed of 53 rpm during the test, which is equivalent to a seeding speed of 16 km/h. Three times each group of tests are administered, and the average of those three results is used to determine the test result. Excel software is used to process the test data as seen in Figure 11. According to Figure 11a, the seed-picking index first rises and then stabilizes as the vacuum degree increases, while the re-picking and miss-picking index first falls and then stabilizes. The vacuum degree between 4 KPa and 8 KPa is chosen as the parameter range because it is an effective interval for meeting the requirements, as can be seen from Figure 11a; according to Figure 11b, the seed-picking index first rises and then falls as the feeder wheel rotation speed increases, while the re-picking and miss-picking index first falls and then rises. The feeder wheel rotation speed between 500 rpm and 620 rpm is chosen as the parameter range because it is an effective interval for meeting the requirements, as can be seen from Figure 11b; according to Figure 11c, the seed-picking index first rises and then falls as the seed-picking angle increases, while the re-picking and miss-picking index first falls and then rises. The seed-picking angle between 8° and 16° is chosen as the parameter range because it is an effective interval for meeting the requirements, as can be seen in Figure 11c. The orthogonal rotation test scheme, consisting of three factors and five levels, was chosen to carry out the test in order to investigate the best combination of the operational parameters for the seed-picking mechanism. The parameter ranges of vacuum degree, feeder wheel rotation speed, and seed-picking angle are 4-8KPa, 500-620rpm, and 8-16°, respectively, based on the results of the single factor tests mentioned above. The factor level codes are shown in Table 1.

Results and Discussion

Multi-factor test results and analysis

The design and results of tests are shown in Table 2.

Parameter optimization

In order to obtain the best parameter combination for the seed-picking mechanism, the regression equations of seed-picking rate, re-picking rate and miss-picking rate were optimized and analyzed using Design-Expert 11 software. The regression equations were optimized and solved using the comprehensive objective function method to establish a mathematical model. Comprehensively considering the conditions and scope of experiment factors of each index, a nonlinear programming mathematical model was obtained

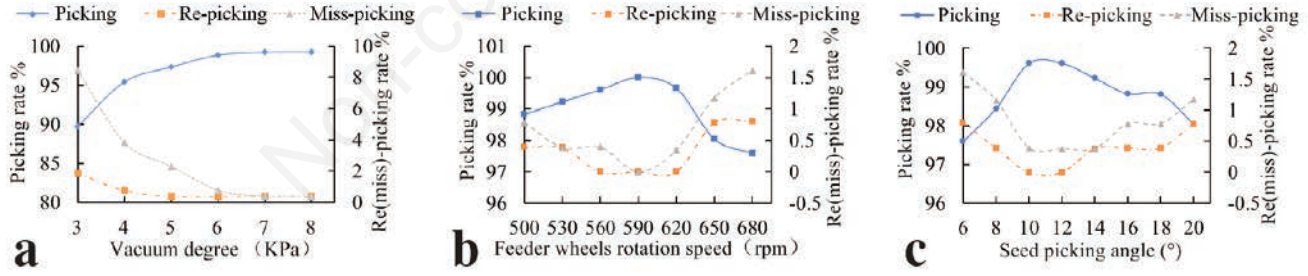

Figure 11. Results of single factor tests. **a**) The feeder wheel rotation speed is 590rpm, and the seed-picking angle is 12°; **b**) the vacuum degree is 6KPa, and the seed-picking angle is 12°; **c**) the vacuum degree is 6KPa, and the feeder wheel rotation speed is 590rpm.

Table 1. Levels of test factors.

Levels	Vacuum degree x_1/KPa	Feeder wheel rotation speed x_2/rpm	Seed-picking angle x_3/km/h
1.682	8.0	620.0	16.0
1	7.2	595.7	14.4
0	6.0	560.0	12.0
-1	4.8	524.3	9.6
-1.682	4.0	500.0	8.0
Step values	1.2	35.7	2.4

$$\begin{cases} \max S(x_1, x_2, x_3) \\ \min H(x_1, x_2, x_3) \\ \min M(x_1, x_2, x_3) \\ \text{s.t.} \begin{cases} 4\text{KPa} \le x_1 \le 8\text{KPa} \\ 500\text{r/min} \le x_2 \le 620\text{r/min} \\ 8^\circ \le x_3 \le 16^\circ \end{cases} \end{cases} \quad (7)$$

The weight of the seed-picking rate is set to the maximum in the Design-Expert 11 software, and the weights of the re-picking rate and the miss-picking rate are set to the minimum, after which the optimization solution is applied: The vacuum degree was 6.89KPa, the feeder wheel rotation speed was 568.95rpm, and the seed-picking angle was 7.6°. The performance indexes obtained under the best parameters were as follows: the seed-picking rate was 99.89%, the re-picking rate was 0, and the miss-picking rate was 0.11%.

Test verification

A verification experiment on the seeding test bench was performed according to the optimal parameter combination of the quadratic regression equations. The vacuum degree was6.89KPa, the feeder wheel rotation speed was 58.95 rpm, and the seed-picking angle was 7.6°. The experiment was repeated 3 times and the experiment results were averaged. The experiment-verified performance index result obtained under the best parameters was as follows: the seed-picking rate was 99.87%, the re-picking rate was 0.01%, and the miss-picking rate was 0.12%. The verification experiment results are similar to the test optimization result and the error rate is ≤5%. The experimental results can meet the technical requirements of corn seeders operating under high-speed sowing conditions.

List of abbreviations

G, gravity of corn seed (°);
F_{N1}, supporting power of primary feeder wheel to seed (N);
F_{N2}, supporting power of auxiliary feeder wheel to seed (N);
F_t, elastic force of feeding wheel on seeds (N);
θ_1, seed-picking angle between primary feeder wheel's support to seed (°);
θ_2, seed-picking angle between auxiliary feeder wheel's support to seed (°);
k, elastic coefficient of finger;
Δx, distortion of finger (mm);
F_c, clamping force of feeder wheels on seed (N);
f_1, friction force of primary feeder wheel to seed (N);
f_2, friction force of auxiliary feeder wheel to seed (N);
μ, friction coefficient between feeder wheels and seed;
m, mass of seed (kg);
R, distance from the center of gravity of corn seed to the center of seed disk (mm);
ω, feeder wheel rotation speed (r/min);
P_a, atmospheric pressure (Pa);
P_0, vacuum degree (Pa);
d, diameter of hole (mm);
N_c, coefficient of supporting force;
T, resultant force of gravity and centrifugal force (N);
N, hole's supporting power to seed (N);
N', supporting force of the hole on the seed along the direction of

Table 2. Design and results of tests..

Test No.	Factors			Indexes		
	x_1	x_2	x_3	Seed-picking rate S (%)	Re-picking rate H (%)	Miss-picking rate M (%)
1	4.8	524.3	9.6	93.49	6.29	0.22
2	7.2	524.3	9.6	94.94	4.86	0.20
3	4.8	595.7	9.6	96.66	3.18	0.17
4	7.2	595.7	9.6	95.10	4.76	0.13
5	4.8	524.3	14.4	96.50	3.30	0.20
6	7.2	524.3	14.4	97.14	2.66	0.20
7	4.8	595.7	14.4	94.48	5.36	0.16
8	7.2	595.7	14.4	94.52	5.34	0.15
9	8.0	560.0	12.0	93.40	6.42	0.18
10	8.0	560.0	12.0	94.94	4.92	0.14
11	6.0	620.0	12.0	94.02	5.76	0.22
12	6.0	620.0	12.0	92.73	7.13	0.13
13	6.0	560.0	16.0	99.71	0.11	0.18
14	6.0	560.0	16.0	99.60	0.22	0.19
15	6.0	560.0	12.0	99.40	0.44	0.17
16	6.0	560.0	12.0	99.65	0.17	0.18
17	6.0	560.0	12.0	99.82	0.00	0.18
18	6.0	560.0	12.0	98.66	1.16	0.18
19	6.0	560.0	12.0	99.51	0.32	0.17
20	6.0	560.0	12.0	98.86	0.98	0.17
21	6.0	560.0	12.0	99.71	0.11	0.18
22	6.0	560.0	12.0	99.81	0.01	0.18
23	6.0	560.0	12.0	99.24	0.58	0.18

the parallel seed disk (N);
J, centrifugal force of seed disk on seed (N);
P, adsorption force on seed (N);
τ, included angle between gravity and centrifugal force which changes with the rotation of the seed disk;
S, seed-picking rate (%);
M, miss-picking rate (%);
H, re-picking rate (%);
N, total number of seeds;
n_1, number of picking seeds;
n_2, number of miss-picking seeds;
n_3, number of re-picking seeds.

Conclusions

First, the planting area of corn is large, the sowing time is short, and the sowing quality directly affects its yield. Therefore, this study takes the seed-picking mechanism of a belt high-speed seed-guiding device for corn as the research object and optimizes the parameters of vacuum degree, feeder wheel rotation speed, and seed-picking angle, which further improves the seed-picking performance of this kind of seed-guiding device, which is of great significance for high-speed sowing of corn in the future.

Second, the movement trajectory of seeds during seed picking at a speed of 12-16 km/h was recorded using high-speed camera technology. When picking seeds normally, the trajectory curve of seeds is parabolic, and there is no jumping point in the whole process. When the seeds are not picked normally because they collide with the feeder wheel, there will be jumping points in the trajectory curve of seeds, and they will be wavy. The single-factor test method was used to obtain the influence law of vacuum degree, feeder wheel rotation speed, and seed-picking angle on the seed-picking rate, re-picking rate, and miss-picking rate. With the increase in vacuum degree, the seed-picking rate first increases and then stays unchanged, and the re-picking rate first lowers and then stays unchanged, in which case the effective range of vacuum degree was 4 KPa to 8 KPa. The seed-picking rate grows and then declines as the feeder wheels rotate faster, and the re(miss)-picking rate decreases and then increases, in which case the effective range of feeder wheel rotation speed was 500 rpm to 620 rpm. The seed-picking rate first rises and then falls as the seed selecting angle rises, while the re(miss)-picking rate first falls and then rises, in which case the effective range of seed-picking angle of 8° to 14°. Finally, the fitted regression equations were optimized and solved using the comprehensive objective function method and Design-Expert 11 software. The optimum combination of picking parameters was obtained and the verification test was carried out under the optimized parameters. The verification test results were as follows: when the vacuum degree was 6.89KPa, the feeder wheel rotation speed was 568.95rpm, and the seed-picking angle was 7.6°. The experiment-verified performance indexes: the seed-picking rate was 99.87%, the re-picking rate was 0.01%, and the miss-picking rate was 0.12%, which achieved the requirements of the corn seeder operating under high-speed sowing conditions.

References

Badua S.A., Sharda A., Strasser R., Ciampitti I. 2021. Ground speed and planter downforce influence on corn seed spacing and depth. Precis. Agric. 22:1154-70.

Hanna H.M., Steward B.L., Aldinger L. 2010. Soil loading effects of planter depth-gauge wheels on early corn growth. Appl. Eng. Agric. 6:551-6.

Garner E.B., Thiemke D.B., Rylander D.J. Mariman N.A., Friestad M.E. 2016. Seeding machine with seed deliver system [P]. United States patent, US 9480199 B2, Nov. 1st, 2016.

Garner E., Friestad M.E., Mariman N.A, Rylander D.J., Thiemke D.B., Liu J.Z., Tevs N.R. 2010. Seed delivery apparatus with sensor and moving member to capture and move seed to a lower outlet opening [P]. United States patent, US2010/0192821, Aug. 5th, 2010.

Jinqing L., Ying Y., Zihui L., Qinqin S., Jicheng L., Zhongyuan L. 2016. Design and experiment of an air-suction potato seed metering device. Int. J. Agric. Biol. Eng. 9:33-42.

Jinwu W., Han T., Jinfeng W., Xin L., Huinan H. 2017. Optimization design and experiment on ripple surface type pickup finger of precision maize seed metering device. Int. J. Agric. Biol. Eng. 10:61-71.

Kaixing Z., Yuanyuan S., Lei L.H., Xianxi L., Xiuyan Z. 2020. Design and test of variable diameter pneumatic drum type bean seed metering device. INMATEH Agric. Eng. 60:9-18.

Kocher M.F., Coleman J.M., Smith J.A., Kachman S.D. 2011. Corn seed spacing uniformity as affected by seed tube condition. Appl. Eng. Agric. 27:177-83.

Li Y., Xing S., Li S., Li L., Zhang X., Song Z., Li F. 2020. Seeding performance simulations and experiments for a spoon-wheel type precision cottonseed-metering device based on EDEM. Mech. Eng. Sci. 2. Available from: https://journals.viserdata.com/index.php/mes/article/view/2615

Liu F., Lin Z., Li D., Zhang T. 2021. Design optimization and performance test of magnetic pickup finger seed metering device. INMATEH Agric. Eng. 137-44.

Liu W., Hu J., Zhao X., Pan H., Lakhiar I.A., Wang W. 2019. Development and experimental analysis of an intelligent sensor for monitoring seed flow rate based on a seed flow reconstruction technique. Comput. Electron. Agric. 164.

Patel S., Bhimani J.B., Gupta P., Yaduvanshi B.K. 2019. Optimization of the operational parameters of a picking-type pneumatic planter using response surface methodology. J. AgriSearch 6.

Qi N., Caiyun L., Hongwen L., Qingjie W., Hongnan H., Zhongcai W., Hongbo Z. 2018. Development of artificial neural network models for seeding performance of a belt-type corn seed metering device. Available from: https://elibrary.asabe.org/abstract.asp?JID=5&AID=49255&CID=det2018&T=1

Sauder G.A., Dill K.R., Dunlap D. L. 2002. Apparatus and method for controlled delivery of seed to an open furrow[P]. United States patent, US 6681706B2, Feb. 26th, 2002.

Wang J., Qi X., Xu C., Wang Z., Jiang Y., Tang H. 2021. Design evaluation and performance analysis of the inside-filling air-assisted high-speed precision maize seed-metering device. Sustainability 13:5483.

Xiong D., Wu M., Wei X., Liu R., Luo H. 2021. Design and experimental study of the general mechanical pneumatic combined seed metering device. Appl. Sci. 11:7223.

Xu P., You Y., Wang D., Sun X., Lv J., Ma W., Zhang X., Ma Z., Lin H. 2020. Optimized design of cone-hole wheel type seed metering device based on EDEM. Am. Soc. Agric. Biol. Eng. Available from: https://elibrary.asabe.org/abstract.asp?JID=5&AID=51423&CID=virt2020&T=1